



# Transition from endemic behavior to eradication of malaria due to combined drug therapies: An agent-model approach

João Sequeira<sup>a,b</sup>, Jorge Louçã<sup>a</sup>, António M. Mendes<sup>c</sup>, Pedro G. Lind<sup>a,d,\*</sup>

<sup>a</sup>Instituto Universitário de Lisboa (ISCTE-IUL), ISTAR-IUL, Av. das Forças Armadas, Lisboa 1649-026, Portugal

<sup>b</sup>Hospital Santa Cruz, Av. Prof. Dr. Reinaldo dos Santos, Carnaxide 2790-134, Portugal

<sup>c</sup>Instituto de Medicina Molecular, Faculdade de Medicina, Universidade de Lisboa, Av. Prof. Egas Moniz, Lisboa 1649-028, Portugal

<sup>d</sup>Department of Computer Science, OsloMet – Oslo Metropolitan University, P.O. Box 4 St. Olavs plass, Oslo N-0130, Norway

## ARTICLE INFO

### Article history:

Received 6 March 2019

Revised 14 September 2019

Accepted 26 September 2019

Available online 27 September 2019

### Keywords:

Malaria spreading

Agent models

Gametocytemia

Transmission control and mitigation

Primaquine

Methylene blue

Ivermectin

## ABSTRACT

We introduce an agent-based model describing a susceptible-infectious-susceptible (SIS) system of humans and mosquitoes to predict malaria epidemiological scenarios in realistic biological conditions. Emphasis is given to the transition from endemic behavior to eradication of malaria transmission induced by combined drug therapies acting on both the gametocytemia reduction and on the selective mosquito mortality during parasite development in the mosquito. Our mathematical framework enables to uncover the critical values of the parameters characterizing the effect of each drug therapy. Moreover, our results provide quantitative evidence of what was up to now only partially assumed with empirical support: interventions combining gametocytemia reduction through the use of gametocidal drugs, with the selective action of ivermectin during parasite development in the mosquito, may actively promote disease eradication in the long run. In the agent model, the main properties of human-mosquito interactions are implemented as parameters and the model is validated by comparing simulations with real data of malaria incidence collected in the endemic malaria region of Chimoio in Mozambique. Finally, we discuss our findings in light of current drug administration strategies for malaria prevention, which may interfere with human-to-mosquito transmission process.

© 2019 Elsevier Ltd. All rights reserved.

## 1. Introduction

Malaria is a parasitic disease, caused by the *Plasmodium* parasite, which is still responsible for the death of nearly half a million individuals every year worldwide (Organization, 2018). *Plasmodium falciparum* (Pf) is the most prevalent form of the malaria parasite in Africa, accounting for 99.7% of all estimated malaria cases in 2017 (Organization, 2018).

While some countries have had reasonable success in rolling back malaria through a well-planned preventive strategy, disease resurgence remains unpredictable. Two types of factors may contribute to such unpredictability. First, “hidden” factors, such as the asymptomatic presence of gametocytes in human systemic circulation, which are the precursors of male and female gametes of the parasite. Migration of just a few asymptomatic human, gametocyte carriers, into particular African regions where the disease is controlled, may act as a potential trigger in malaria outbreaks (Lee et al., 2010; Pagès et al., 2018). The presence of gametocytes may

be mitigated through the application of gametocidal drugs, such as primaquine or methylene blue.

Second, malaria transmission can be promoted due to the intrinsic heterogeneity in human demography and mosquito behavior (Lloyd and May, 1996). For example, in a potential outbreak, human fatality rate may rise out of proportion due to the weaker immunity of local populations from reduced exposure to the parasite (Tyrrell et al., 2017). Or, in regions under anti-malaria massive drug administration, drug-resistant parasite strains can develop and consequently, through human migratory phenomena, they may be imported into areas of near eradication, locally strengthening malaria transmission (Lee et al., 2010; Pagès et al., 2018; DePina et al., 2018).

Although the decisive role these factors can play on malaria transmission mechanisms is well established, the impact on malaria transmission resulting from the combined effect of different drug therapies in heterogeneous populations is still not fully understood.

The life cycle of Pf may be summarized as follows. The malaria vector, the mosquito, *Anopheles spp.*, usually lives, mates and feeds within a few miles distance from its birthplace (Kaufmann and

\* Corresponding author.

E-mail address: [pedro.lind@oslomet.no](mailto:pedro.lind@oslomet.no) (P.G. Lind).

Briegel, 2004). To become infectious to humans, the mosquito needs to survive 10 or more days after feeding on a *Pf* gametocyte carrier. This time period is required to complete parasite sporogonic development inside the mosquito (Eckhoff, 2011), after which, mosquito-to-human transmission becomes possible. Therefore, strict gametocidal drugs may not only block human-mosquito transmission, but can also have a strong impact on it. Other drug agents, such as ivermectin, have become a promising antimalarial interventions due to its anophelocide properties, preventing parasite's maturation inside the mosquito (Chaccour et al., 2010; Kobylinski et al., 2012; Omura and Crump, 2017). It is known that mosquitoes, feeding on human hosts under ivermectin treatment, have a considerably lower life expectancy, with a large fraction of mosquito deaths within 4 days after the blood meal (Chaccour et al., 2010; Kobylinski et al., 2012; Ouédraogo et al., 2015).

Moreover, interventions including mass administration of ivermectin in prevention of several other African endemic parasites have resulted in a significant reduction of malaria incidence on those regions (Alout et al., 2014; Mendes et al., 2017; Kobylinski et al., 2011).

To tackle the specific problem related with malaria transmission in a human community, several mathematical models have been proposed. Early models, such as those by Ross and McDonald, were deterministic (Ross, 1915; Macdonald, 1957), having nonetheless a significant relevance in malaria epidemiology (Dietz et al., 1974; Koella, 1991; Ngwa and Shu, 2000; Mandal et al., 2011; Chitnis et al., 2012; 2018; White et al., 2009) and being since then refined. More recent variants have been developed with the help of modern satellite imaging, precise weather and geographical information, computational agent-based modeling, and advanced statistics, such as hidden Markov processes, time-series analysis and big-data approaches (Eckhoff, 2011; Chitnis et al., 2012; Depinay et al., 2004; McKenzie and Bossert, 2005; Gaudart et al., 2009; Kamgang and Tchoumi, 2015; Ewing et al., 2016; Sarkar and Chatterjee, 2017). In particular, agent-based models strengthen the importance of malaria simulation for disease prevention (Eckhoff, 2011; Gerardin et al., 2015; Smith et al., 2018). Based on the classical susceptible-infected (SI) model by Kermack and McKendrick, stochastic modeling approaches were also proposed, with the aim of better implementing the uncertainties inherent to the disease dynamics (Ferrão et al., 2017a).

Epidemiological field data of malaria transmission is commonly presented as human monthly or weekly disease incidence (Ferrão et al., 2017a; Aregawi et al., 2014), while mosquito infection rates are obtained from data collected through the use of mosquito trapping devices (Bomblies et al., 2009). However, since both are important to understand the transmission dynamics, one should account for the combined effect of human and mosquito infection prevalence.

In this paper, we introduce an agent-based model of *Pf* malaria endemic/epidemic behavior, incorporating both human-to-mosquito and mosquito-to-human transmission processes. We parameterize some of the most important biological aspects of disease transmission, focusing mainly in the parameters describing the reduction of gametocytemia prevalence in the human host and the extension of ivermectin administration in the population. The model assumes a typical isolated African village with limited access to drug therapy and is based on discrete Markov processes describing the succession of human-mosquito encounters, which are implemented through a Monte Carlo algorithm. Tuning the parameter defining gametocytemia inside the human host, or the parameter controlling the fraction of the human population under ivermectin treatment, we uncover a phase transition between disease eradication and epidemic prevalence. In both cases, the transition is sensitive to minor changes in the parameters, and through

mathematical analysis, we are able to predict critical values separating the two phases, eradication and endemic prevalence.

We start in Section 2 by describing the agent model and the main parameters driving *Pf* gametocytemia and human-mosquito infection dynamics. In Sections 3 and 4 we present respectively the main results and describe the validation procedure using data sets from the endemic region of Chimoio in Mozambique. In Section 5 we discuss the impact of our results on possible clinical and medical strategies, and conclude the paper.

## 2. Agent model for human-to-mosquito and mosquito-to-human transmission

We consider a system of  $M = 4000$  mosquitoes and  $H = 2000$  human individuals, where each population is divided into a number of healthy and another of infected individuals, represented by  $H_0$  and  $M_0$  and by  $H_i$  and  $M_i$  respectively:  $H = H_0 + H_i$  and  $M = M_0 + M_i$ . Although in reality, the density of mosquitoes is much higher, we model the amount of mosquitoes as the effective fraction of the overall mosquito mass, imposing an average of two bites per day for each mosquito.

The chosen values of each parameter are given in Table 1, and the algorithm keeps track of all attributes for each agent, human or mosquito, in a particular age, time since infection, and immunity status. Notice that only two parameters are modulated, namely the fraction  $p_{iv}$  of the human population subjected to ivermectin treatment and the effectiveness of gametocidal drugs, measured as the number  $\tau_g$  of days of positive gametocytemia. All other parameters are kept at constant values and their values were chosen according to previous studies.

The flowchart describing the computer implementation of the agent model is sketched in Fig. 1 and is described as follows. The algorithm simulates a total time interval of 30 years and it starts by evaluating each individual, to ascertain if it became cured or not. In the case of human individuals the recovered rate  $q_h$  is a fixed value, dependent on the average time  $\tau_c$  it takes for one individual to be cured,

$$q_h = \frac{1}{\tau_c}. \quad (1)$$

In the case of mosquitoes, there is no explicit recovery rate. Every dead mosquito is replaced by a new healthy mosquito. As such, the mosquito recovery rate equals its mortality rate  $q_m$ . The mosquitoes' mortality is determined by its natural life expectancy,  $\tau_m$ , the fraction  $p_{iv}$  of human with whom the mosquito interacts that is under ivermectin treatment and the life expectancy  $\tau_m^{(iv)}$  of a mosquito with exposure to ivermectin:

$$q_m = (1 - p_{iv}) \frac{1}{\tau_m} + p_{iv} \frac{1}{\tau_m^{(iv)}}. \quad (2)$$

The two rates,  $q_h$  and  $q_m$ , are not directly implemented in the agent model. Instead, we impose a maximum time of human infection of  $\tau_d = 150$  days and a minimum time of 25 days, uniformly distributed, yielding an average human infectious period of  $\tau_c = 87.5$  days, a maximum mosquito life time of 40 days and a minimum life time of 0 days, uniformly distributed, yielding an average life expectancy of one mosquito  $\tau_m = 10$  days, as well as a probability  $g_{iv} = 0.5$  of one mosquito to die from feeding on a human host under ivermectin treatment. In case of an infectious mosquito bite in an infected human host, a human reinfection or super-infection occurs<sup>1</sup> and the disease time of that human individual is reset to half of the present disease time. Beyond 5 years

<sup>1</sup> Persistent reinfection is defined as a new contact between an infected human host and an infected mosquito, during the time period of active infection. In practice, since the average time of infection in one human is 87.5 days, one human host may reacquire a new malaria infection within three months after the initial

**Table 1**

Parameters of the agent-based model for malaria spreading within two interacting communities of human individuals and mosquitoes. The values chosen for the simulations are taken, based in previous studies.

Tunable parameters	Symbol	Value	References
Probability of ivermectin treatment	$p_{iv}$	0.00–0.10	-
Duration of positive gametocytemia	$\tau_g$	58–90 (days)	(Macdonald, 1957; Gaudart et al., 2009; Karl et al., 2011)
FIXED PARAMETERS			
	SYMBOL	VALUE	
Number of human individuals	$H$	2000	(Mandal et al., 2011; Chitnis et al., 2012; Gaudart et al., 2009)
Number of (female) mosquitoes	$M$	4000	(Mandal et al., 2011; Chitnis et al., 2012; Gaudart et al., 2009)
Average number of bites from one mosquito	$n_b$	2 (per day)	(Macdonald, 1957; Mandal et al., 2011; Gaudart et al., 2009; Karl et al., 2011) (Jindal, 2017)
Total simulation time	-	30 (years)	-
Maximum time of human infection (including time of parasite development)	$\tau_d$	150 (days)	(Macdonald, 1957; Mandal et al., 2011; Felger et al., 2012; Bretscher et al., 2015)
Minimum time of human infection (including time of parasite development)	$\tau_0$	25 (days)	(Macdonald, 1957; Mandal et al., 2011; Felger et al., 2012; Bretscher et al., 2015)
Average human infectious period, cf. Eq. (1)	$\tau_c$	87.5 (days)	(Macdonald, 1957; Mandal et al., 2011; Felger et al., 2012; Bretscher et al., 2015)
Maximum life time of one mosquito	$\tau_{max}$	40 (days)	(Macdonald, 1957; Mandal et al., 2011)
Minimum life time of one mosquito	$\tau_{min}$	0 (days)	(Macdonald, 1957; Mandal et al., 2011)
Mosquito death probability from feeding in human with ivermectin	$g_{iv}$	0.5	(Chaccour et al., 2010; Kobylinski et al., 2012; Ouédraogo et al., 2015; Alout et al., 2014)
Time needed to acquire immunity due to persistent reinfection	-	5 (years)	(Macdonald, 1957; Gaudart et al., 2009; Gurarie et al., 2012; Ngonghala et al., 2016) (Filipe et al., 2007; Doolan et al., 2009; Coffeng et al., 2017; Ngonghala et al., 2014)
Time needed for losing immunity (in the absence of infection)	-	2 (years)	(Macdonald, 1957; Gaudart et al., 2009; Gurarie et al., 2012; Ngonghala et al., 2016) (Filipe et al., 2007; Doolan et al., 2009; Coffeng et al., 2017; Ngonghala et al., 2014)
Probability of protection from LLIN, ITN and IRS barriers	$u$	0.25	(Karl et al., 2011; Organization, 2013; Ngonghala et al., 2016; Korenromp et al., 2016)
Single episode mosquito mortality of LLIN/ITN/IRS protection	$g_{irs}$	0.50	(Eckhoff, 2011; Karl et al., 2011; Organization, 2013; Ngonghala et al., 2016)
Probability of a mosquito bite in the low season	$p_{ls}$	0.5	(Ferrão et al., 2017a; 2017b)
Probability of a mosquito bite in the high season	$p_{hs}$	1	(Ferrão et al., 2017a; 2017b)
Fraction of humans among all animals bitten (anthropophilic factor)	$p_Q$	0.9	(Killeen et al., 2016; Hasyim et al., 2018)
Duration of the gonotrophic reproductive cycle	$\tau_s$	4 (days)	(Eckhoff, 2011; Organization, 2013)
Duration of the high transmission season	$\delta_s$	150 (days)	(Ferrão et al., 2017a; 2017b)
Probability of human infection after infectious mosquito bite	$k_h$	0.20	(Karl et al., 2011; Ngonghala et al., 2016; 2014; Ermert et al., 2011)
Probability of mosquito infection after bite in infectious human	$k_m$	0.20	(Annan and Mukinay, 2017; Laurens et al., 2013; Lyke et al., 2010) (Karl et al., 2011; Ngonghala et al., 2016; 2014; Ermert et al., 2011)
Time for parasite development in the mosquito	$\tau_{lm}$	10 (days)	(Annan and Mukinay, 2017; Laurens et al., 2013; Lyke et al., 2010)
Time for parasite development to gametocyte stage inside human host	$\tau_{lh}$	10 (days)	(Mandal et al., 2011; Chitnis et al., 2012) (Mandal et al., 2011; Karl et al., 2011)
Probability of full protection due to acquired immunity	$v_{max}$	0.3	(Macdonald, 1957; Filipe et al., 2007; Doolan et al., 2009; Coffeng et al., 2017)
Fraction of children (age < 5 years) in the population	-	0.12	(Gaudart et al., 2009; Filipe et al., 2007; Doolan et al., 2009)
Probability of positive gametocytemia in children	-	0.70	(Gaudart et al., 2009; Felger et al., 2012)
Average number of humans that die, per year (global causes)	$\mu_h$	0.015	(Organization, 2018; Mandal et al., 2011; Ferrão et al., 2017b)
Seasonality overall bite probability	$s$	0.7055	(Ferrão et al., 2017a; 2017b)
Initial protection probability from acquired immunity	$\nu_0$	0.1	(Macdonald, 1957; Gurarie et al., 2012; Filipe et al., 2007; Doolan et al., 2009)
Probability of mosquito bite from surviving mosquitoes past latency	$\pi_{lm}$	0.686	(Eckhoff, 2011; Macdonald, 1957; Chitnis et al., 2012; Gaudart et al., 2009) (Karl et al., 2011)
Probability of daily mosquito mortality (general causes)	$q_m$	0.10	(Eckhoff, 2011; Macdonald, 1957; Chitnis et al., 2012; Gaudart et al., 2009) (Karl et al., 2011; Organization, 2013)
Probability of human disease daily recovery ( $= \frac{1}{\tau_c}$ )	$q_h$	0.011	(Macdonald, 1957; Mandal et al., 2011; Karl et al., 2011)

of persistent human reinfections, the human host acquires maximum immunity and after 2 years with no infection events, the host loses immunity completely.

In case the mosquito succeeds in overcoming the barrier protection, the algorithm starts to ascertain if transmission will take

place or not. This is done by computing the probability  $r$  for one mosquito and one human individual or other animal to contact through one bite, which is given by

$$r = \left( (1 - s)p_{ls} + sp_{hs} \right) \frac{p_Q}{\tau_s}, \tag{3}$$

where  $s$  is the fraction of time in the year with high disease transmission (percentage of time in rainy season),  $p_{ls}$  and  $p_{hs}$  represent the fractions of the year covered by the low and high

infection episode, thus perpetuating disease transmission as well as immunity individual acquisition.

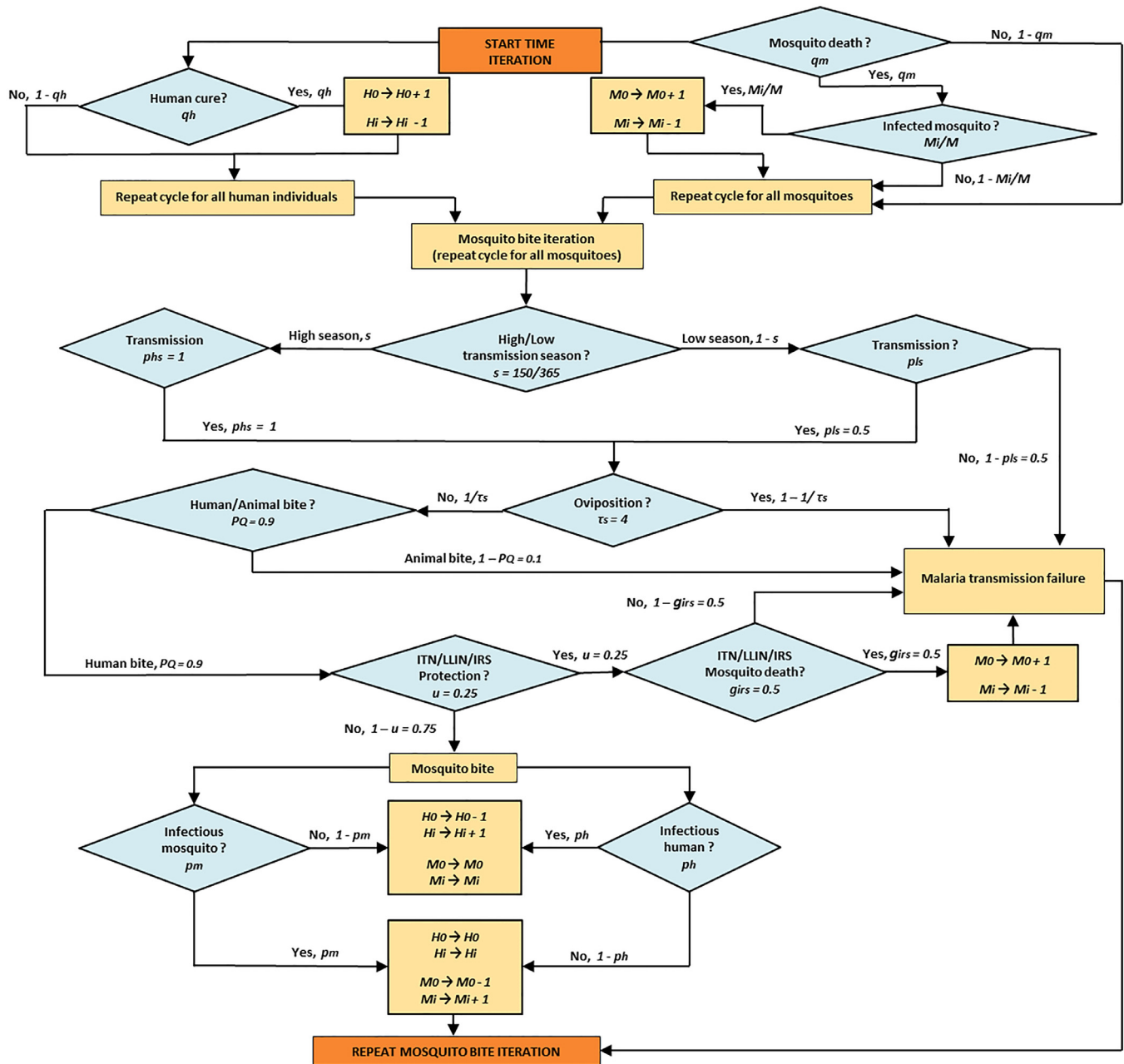


**Fig. 1.** Flowchart of the agent-based model for human-mosquito interaction to reproduce scenarios of malaria spreading. Probabilities  $q_h$  and  $q_m$  are given in Eqs. (1) and (2) respectively. The other probabilities are given in Table 1. The probability for infecting a human or a mosquito depends on  $p_h$  and  $p_m$ , given in Eqs. (4) and (5) respectively, and also on additional details concerning the dynamics of immunity acquisition of each human individual and the fraction of the human population composed by children (see text).

seasons respectively,  $p_Q$  is the fraction of humans among all animals able to be bitten by one mosquito within the geographical region covered by the mosquito community, and  $\tau_s$  is the duration of the gonotrophic reproductive cycle. In the agent model, we use values provided in previous studies, namely  $p_{hs} = 1$ ,  $p_Q = 0.9$  and  $\tau_s = 4$  days. In our model a high value of human blood index was assumed, corresponding to a strong anthropophilic mosquito feeding, more typical of *Anopheles gambiae sensu stricto* (s.s.) or *An. funestus*, and different from *An. arabiensis*. Moreover, inspired in Mozambique seasonality (Ferrão et al., 2017a; 2017b), we consider 150 days for the duration of the high transmission season, i.e.  $s = 150/365$ . Notice that during transmission season, one considers a non-zero probability of transmission; in this way, disease transmission may occur during the whole

year, although with higher intensity during the high-transmission season.

Upon updating the number of healthy humans individuals and mosquitoes, the algorithm proceeds to generate one mosquito bite attempt. Here one introduces the probability  $u = 0.25$  that long lasting insecticide-impregnated nets (LLIN), insecticide-impregnated nets (ITN) or indoor residual spraying (IRS) may protect human hosts from mosquito bites. This parameter represents the degree of human population protection resulting from LLIN, ITN or IRS preventive measures, and simulates the probability of mosquito bite failure due to protective barrier, assuming the form  $(1 - u)$  to be included in the final mosquito bite probability defined as  $r(1 - u)$  - see Fig. 1. Additionally, we also introduce the effect of barriers in killing the mosquito during the bite attempt. In



the model, the probability of mosquito mortality induced by protective barriers is 0.5.

In the case one of the above factors succeeds, malaria transmission fails. In case all barriers fail, the algorithm finds one mosquito-human interaction through one bite. If the two interacting agents are infected or none of them is, both populations remain unchanged and the algorithm starts the next iteration. If only one individual (either human or mosquito) is infected, the algorithm ascertains if malaria transmission is successful.

The probability  $p_h$  for such single bite to effectively transmit the parasite from an infected mosquito to a healthy human depends on four factors, namely (i) the fraction  $M_i/M$  of infected mosquitoes, the probability  $k_h$  to get infected from one single mosquito bite<sup>2</sup>, the probability  $w_m$  that the mosquito is ready to transmit the parasite, and the probability  $\nu$  of human individual immunity protection, yielding

$$p_h = \frac{M_i}{M} k_h w_m (1 - \nu) \quad (4)$$

and similarly, the probability for one single bite to effectively transmit the parasite from an infected human to a healthy mosquito is

$$p_m = \frac{H_i}{H} k_m w_h. \quad (5)$$

The probability  $w_m$  is obtained from the fraction of surviving mosquitoes past the period of parasite development, i.e.

$$w_m = e^{-q_m \tau_{lm}}, \quad (6)$$

where the parameter  $\tau_{lm}$  is the period of parasite development in the mosquito. As for  $w_h$  it measures the fraction of time of the duration of positive gametocytemia from the maximal period of human infection,

$$w_h = \frac{\tau_g}{\tau_d}, \quad (7)$$

where  $\tau_d$  is the maximal period of human infection and  $\tau_g$  is the duration of positive gametocytemia.

In the agent model we fix  $k_m = k_h = 0.2$ ,  $\tau_{lm} = \tau_{lh} = 10$  days and  $\tau_d = 150$  days. Notice that the duration of positive gametocytemia is a tunable parameter used for varying  $w_h$ , which will be one of the important parameters below. Since  $\tau_d$  takes values between 58 and 90 days (see Table 1), the probability  $w_h$  varies between 0.387 and 0.733<sup>3</sup>, a range that includes a phase transition from malaria eradication to malaria endemic behavior.

Notice that a higher gametocyte density will result in higher human-to-mosquito transmission efficiency. Consequently, the concept of gametocytemia reduction is considered equivalent to the effects of treatment with gametocidal agents such as primaquine or methylene blue.

The agent model implements three additional ingredients that are not usually taken into account in simulation of malaria transmission dynamics.

First, in the present model we simulate the use of ivermectin in a fraction of the human population ( $p_{iv}$ ), assuming a global

ivermectin-related mosquito fatality rate ( $g_{iv}$ ) of 0.5. Ivermectin inhibits sporogony in the mosquito having a partial blocker effect on human-to-mosquito transmission. We used this mechanism for defining ivermectin biodynamic in our computational model.

Second, to consider the effect of acquired immunity to malaria infection. Acquired immunity  $\nu$  against malaria changes according to the history of infection and the genetic traits of a particular human individual. The value of  $\nu$  can increase in the case of repeated reinfections, or decrease, in case no infection is observed during a certain time. The time to acquire protective immunity after every infection episode is typically longer than that of the immunity loss. We consider that if the human host does not contact with the parasite during two years, he/she loses the acquired immunity against the parasite, while maximal immunity is gained after 5 years with persistent reinfection. Moreover, maximum protective immunity is different from complete protective immunity, as a human cannot be more than 30% immune,  $\nu_{max} = 0.3$ . Notice that, the acquired immunity, parameterized through  $\nu$ , is incorporated in parameter  $p_h$  - see Eq. (4) - which is indicated in one of the boxes in the flowchart of Fig. 1.

Third, the extreme vulnerability to malaria infection of children under 5 years of age is a well-known critical factor in the disease morbidity and mortality. We therefore consider additional effects for the subgroup of children in the human population. A simplified age effect is considered: the fraction of children under 5 years of age represents 12% of the total human population, and for those children immunity is considered to be absent, with a higher gametocytemia prevalence during disease duration, namely during 70% of the time (Gaudart et al., 2009; Bretscher et al., 2015; Gurarie et al., 2012; Filipe et al., 2007; Doolan et al., 2009; Coffeng et al., 2017).

Malaria unrelated human mortality, is also considered in our model. However, its magnitude is considered low, namely 0.015 cases per year, i.e. it has negligible effects in disease transmission. The system is always initialized with a fraction of infected mosquitoes of 1%, a fraction of infected humans of 5% and an initial acquired immunity of  $\nu_0 = 0.1$  for every human individual<sup>4</sup>.

Our model has its limitations. Some variables can be modelled with distributions which are derived from standard mathematical derivations, such as the time for human disease recovering, treated here as a stochastic variable exponentially distributed. Other random variables, however, not necessarily related with exponentially decaying processes were taken as uniformly random variables, e.g. variables related to mosquito biting behavior, human disease duration or gametocytemia occurrence, since no other forms of statistical distribution have been firmly established. Notice that the risk of using other distributions such as Gaussian, Poisson or Gamma distribution, can lead to scenarios and transition features different from those reported below, but such assumptions need further investigations and are out of the scope of the present work. Another simplification is the parameterization of ivermectin. It is known that, ivermectin is an anti-mosquito measure with a fast decaying rate: mosquitoes taking a blood meal containing this drug have an enhanced mortality rate that is directly related to the ivermectin concentration present in the blood. This fact is not incorporated in the present model, similarly to other studies in this topic (Kobylinski et al., 2012; Ouédraogo et al., 2015).

### 3. Assessing the effect of drug therapies

In this section, we address separately the effect of gametocidal drugs and of ivermectin, choosing proper values for generating each of three possible scenarios:

<sup>2</sup> The value of the probability to get infected from one single bite, either for humans as for mosquitoes, is given by the inverse of the number of infected mosquito bites necessary to infect one human or one mosquito and it estimated from controlled malaria infection, in laboratory settings (Laurens et al., 2013; Lyke et al., 2010).

<sup>3</sup> Gametocyte detection threshold by light microscopy usually retrieves measurements between 5 and 10 gametocytes per  $\mu\text{L}$ . But with current molecular detection methods, that threshold may be as low as 0.1 per  $\mu\text{L}$  (Karl et al., 2011). It is assumed that during the period of human disease, gametocytemia will occur according to a random stochastic process, with a predefined probability of human-to-mosquito transmission at every mosquito bite in the range of admissible values (Karl et al., 2011; Kuehn and Pradel, 2010).

<sup>4</sup> Except children under 5 years of age, who are assumed to have an acquired immunity of 0.0.

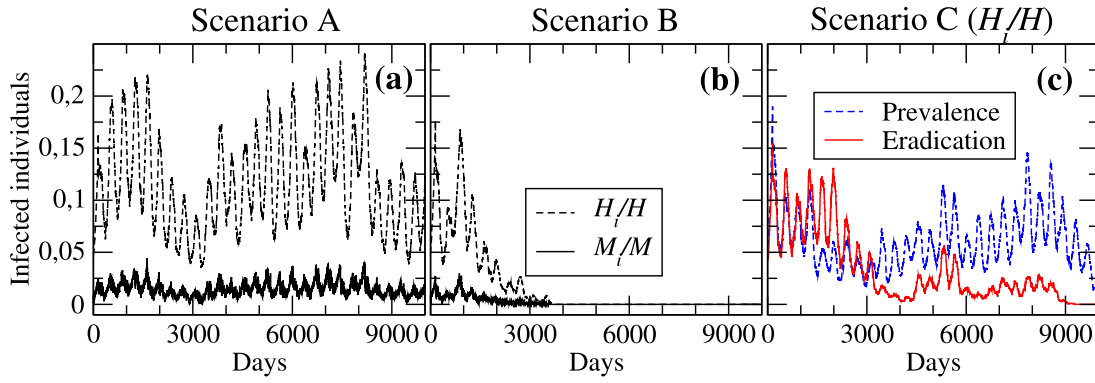


**Fig. 2.** Illustration of the three scenarios tuned by gametocytemia parameter  $w_h$ : (a) Scenario A, disease epidemic prevalence ( $w_h = 0.453$ ), (b) Scenario B, disease eradication ( $w_h = 0.387$ ), and (c) Scenario C, transition between prevalence and eradication ( $w_h = 0.420$ ). In all cases  $p_{iv} = 0$ .

- Scenario A: Disease endemic/epidemic prevalence ( $H_i > 0$  and  $M_i > 0$ ).
- Scenario B: Disease eradication ( $H_i = 0$  and  $M_i = 0$ ).
- Scenario C: Critical phase transition between endemic disease and eradication, where some of the simulations evolve to disease eradication, while other to epidemic prevalence.

### 3.1. The role of gametocytemia in disease dynamics

We define the effect of ivermectin as null at  $p_{iv} = 0$  and generate illustrative examples of each scenario. For Scenario A, we consider  $\tau_g = 68$  days of gametocytemia yielding a value of  $w_h = 68/150 = 0.453$ , for Scenario B we consider  $\tau_g = 58$  days of gametocytemia, i.e.  $w_h = 0.387$ , and for Scenario C  $\tau_g = 63$  days ( $w_h = 0.420$ ). Results are shown in Fig. 2.

Fig. 2a illustrates Scenario A, where both human and mosquito communities evolve in periodic cycles, reflecting the seasonal character of malaria incidence, changing between low and high transmission seasons. Here, none of the infected communities converges to eradication. In Fig. 2b one observes the opposite: both communities eventually get cured with no cases of infection. In the plotted example this occurs after one seasonal cycle (1 year). For the Scenario A, we obtained  $12\% \pm 4\%$  of infected humans and  $1.5\% \pm 0.7\%$  of infected mosquitoes, while for the Scenario B, we obtained  $1\% \pm 3\%$  of infected humans and  $0.2\% \pm 0.4\%$  of infected mosquitoes.

In Fig. 2c we observe the intermediate situation, between endemic prevalence and eradication. Two different outcomes occur at identical gametocytemia levels: in blue dashed lines we plot the evolution of human community in a simulation where the disease persists for more than 30 years and in red solid lines, one observes the resulting community evolution towards a state of eradication, after around 20 years. This intermediate scenario occurs for  $w_h \sim 0.42$ .

For the eradication case of Scenario C we obtained  $3\% \pm 3\%$  of infected humans and  $0.3\% \pm 0.4\%$  of infected mosquitoes, and for the prevalence situation,  $6\% \pm 3\%$  of infected humans and  $0.7\% \pm 0.4\%$  of infected mosquitoes.

Two important features must be addressed at this point. First, the time span needed for eradication at the transition value is considerably larger than for values below the transition. This is a common feature in critical phase transitions (Stanley, 1971).

Second, the different outcomes from Scenarios A, B and C result from small changes in the time of gametocytemia prevalence: the differences between scenarios A, B and C are not greater than 5 days, which represents gametocytemia differences of  $\pm 3.3\%$ . Consequently, small changes in gametocytemia status may result in

significant changes on the level of epidemic outcome, a feature that shows the importance of gametocytemia in controlling malaria transmission.

To better uncover the transition from endemic prevalence to eradication due to gametocytemia control, we generate 10 different realizations for a set of different  $w_h$  values within a range covering all three scenarios. Results are shown in Fig. 3a. As one sees, while for Scenarios A and B, all realizations converged to the same state, prevalence or eradication respectively, for Scenario C one fraction of the realizations ended in endemic prevalence while the rest converged to eradication. Therefore, we argue that there is a critical value of gametocytemia days that guarantees full recovery of the community.

A quantitative approach for estimating this transition gametocytemia value is to approximate the transition curve in Fig. 3a by a step function of the form

$$F_g(w_h) = \frac{1}{1 + \left(\frac{w_h^{(t)}}{w_h}\right)^{\alpha_g}}, \quad (8)$$

yielding an estimate for the transition gametocytemia value of  $w_h^{(t)} = 0.42$  and for the exponent  $\alpha_g = 32$ . The functional form in Eq. (8), is a kind of Fermi-function, which, in this case, enables to parameterize the transition from eradication to prevalence with two single parameters, a critical value  $w_h^{(t)}$  for which  $F_g(w_h^{(t)}) = 1/2$ , and a transition “length”  $\alpha_g$  which controls how sensitive the transition is with respect to variations of gametocytemia around the critical value.

In real situations of malaria epidemics, there are several difficulties in properly determining the annual malaria incidence<sup>5</sup>, which is an adequate measure for evaluating the gravity and extension of the epidemic. Through simulations, the annual malaria incidence can not only be more easily calculated, but it is also possible to investigate how it relates with other variables. As shown in Fig. 3b, we observe a clear linear relation between the average malaria incidence  $I$  and the gametocytemia parameter  $w_h$ . In the plot, for each value of positive gametocytemia  $w_h$  we obtained the average of the annual malaria incidence over 10 different simulations. A linear regression of the simulation results yields

$$I = -202 + 508w_h, \quad (9)$$

with a coefficient of determination of  $r^2 = 0.9983$  and a  $p$ -value of  $P < .001$ . Notice that for  $w_h < 202/508 \lesssim w_h^{(t)}$ , close to obtained

<sup>5</sup> Annual malaria incidence represents the instant expected average of malaria incidence per 100 inhabitants during one full year, if transmission conditions remain unchanged.

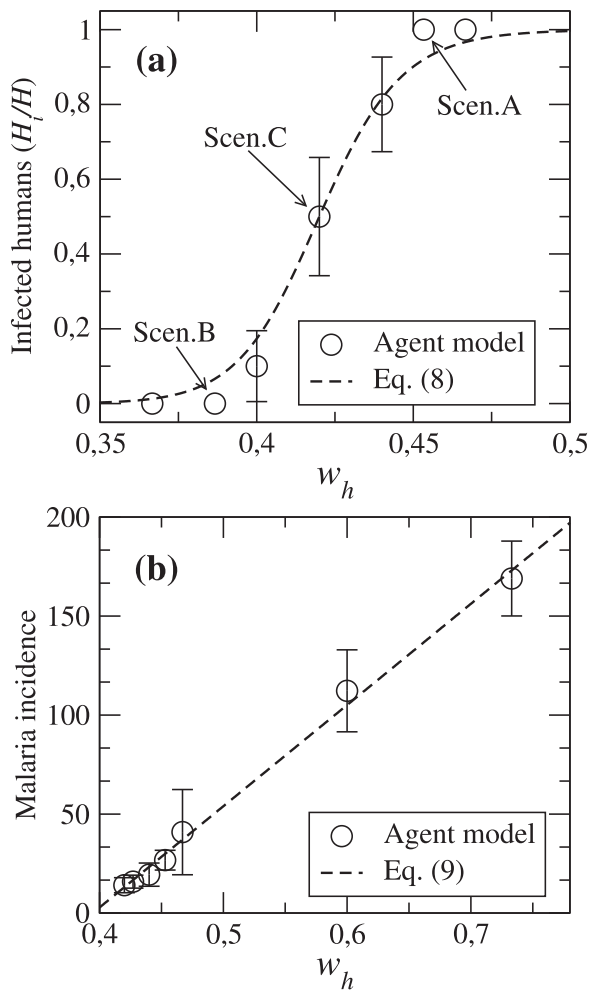


**Fig. 3.** (a) Probability of epidemic outcome with changing gametocytemia duration at phase transition. The three scenarios illustrated in Fig. 2 are indicated with arrows. The function in Eq. (8) is plotted with dashed line. The fraction of infected humans is averaged over 10 realizations for each value of  $w_h$ . (b) Annual malaria incidence per 100 habitants and its correlation with the positive gametocytemia  $w_h$ . Correlations were computed by averaging over 10 realizations for each value of  $w_h$ .

transition value of gametocytemia, the annual incidence is negative, meaning that the system converges to a scenario of disease eradication. Only for values above the transition value one observes a positive malaria incidence.

### 3.2. The role of ivermectin in transmission prevention

To investigate the role of ivermectin we fix the value for the time of positive gametocytemia, since it appears to be independent from human-to-mosquito transmission efficiency. We choose a stable epidemic background with 90 days of gametocytemia, corresponding to  $w_h = 0.6$ . To investigate the mosquito mortality due to ivermectin, we first focus on three different values of the fraction of human population under ivermectin treatment, namely  $p_{iv} = 0, 0.05, 0.1$ . Each of these three values illustrates one of three different regimes, respectively (i) absence of ivermectin treatment, (ii) weak ivermectin administration and (iii) moderate ivermectin administration.

Our results show that, while in the absence of ivermectin administration the mosquito mortality during parasite development is 79.6%, for  $p_{iv} = 0.05$  the mortality increases to 84.4% and for  $p_{iv} = 0.1$  to 88.1%. In the case of bite failure due to barrier

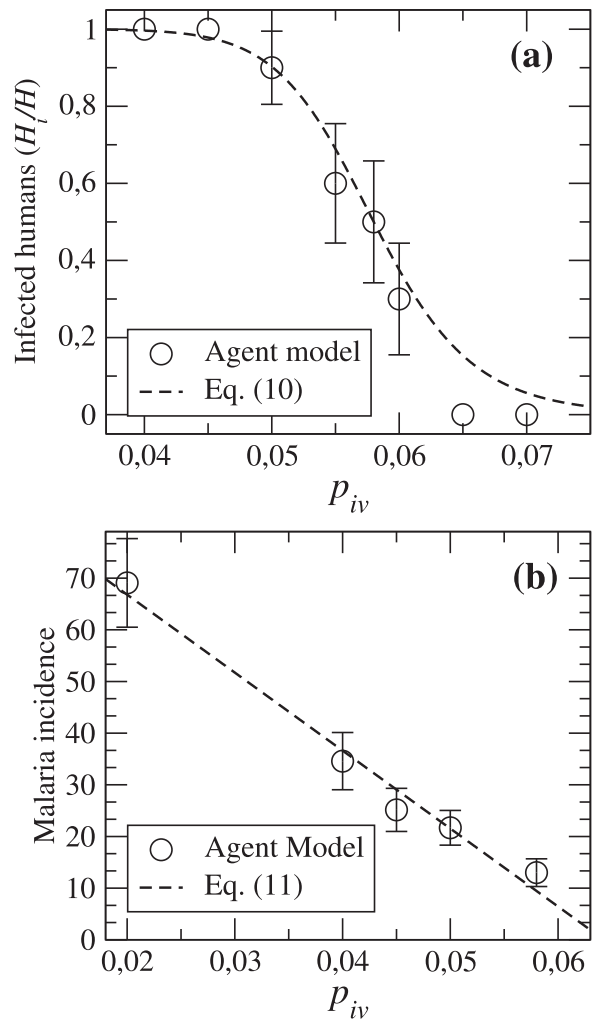


**Fig. 4.** (a) Probability of epidemic outcome with probability of ivermectin treatment at phase transition, and approximate fit function. Here we run 10 trials for each value of  $p_{iv}$ . (b) Annual malaria incidence per 100 habitants and correlation with ivermectin treatment probability ( $p_{iv}$ ). Positive gametocytemia is fixed at  $w_h = 0.6$ .

protection, the mosquito mortality is considered relevant, and set at  $g_{irs} = 0.5$ <sup>6</sup>.

We have also observed that, in the case of ivermectin random usage in 5% of the population, disease eradication may occur roughly 20 years later. But if ivermectin is administered to 10% of the human population, a disease eradication outcome may be possible much earlier (less than 4 years). Moreover, the administration of ivermectin induces a reduction in the frequency of healthy mosquito bites in an infected human (not shown).

Varying the fraction  $p_{iv}$  uncovers also a continuous phase transition from prevalence to eradication. See Fig. 4a. Differently from the transition by gametocytemia variation, here the phase transition is only visible for high gametocytemia levels, typically  $w_h = 0.6$  or larger. A possible explanation for this is the strong inhibitory effect of ivermectin on human-to-mosquito disease transmission.

In Fig. 4a, a phase transition from epidemic prevalence to disease eradication can be observed. Here, the critical value of the hu-

<sup>6</sup> There is no precise knowledge concerning the probability for the mosquito to die due to ITN, IRS or LLIN barriers. We assumed a value of 0.5, which together with a coverage of ITN of 25%, results in a global mortality due to ITN barriers of  $0.25 \times 0.5 = 0.125$ . This value is probably below the real value, since in several African countries the LLIN/ITN/IRS coverage may be as high as 80%.

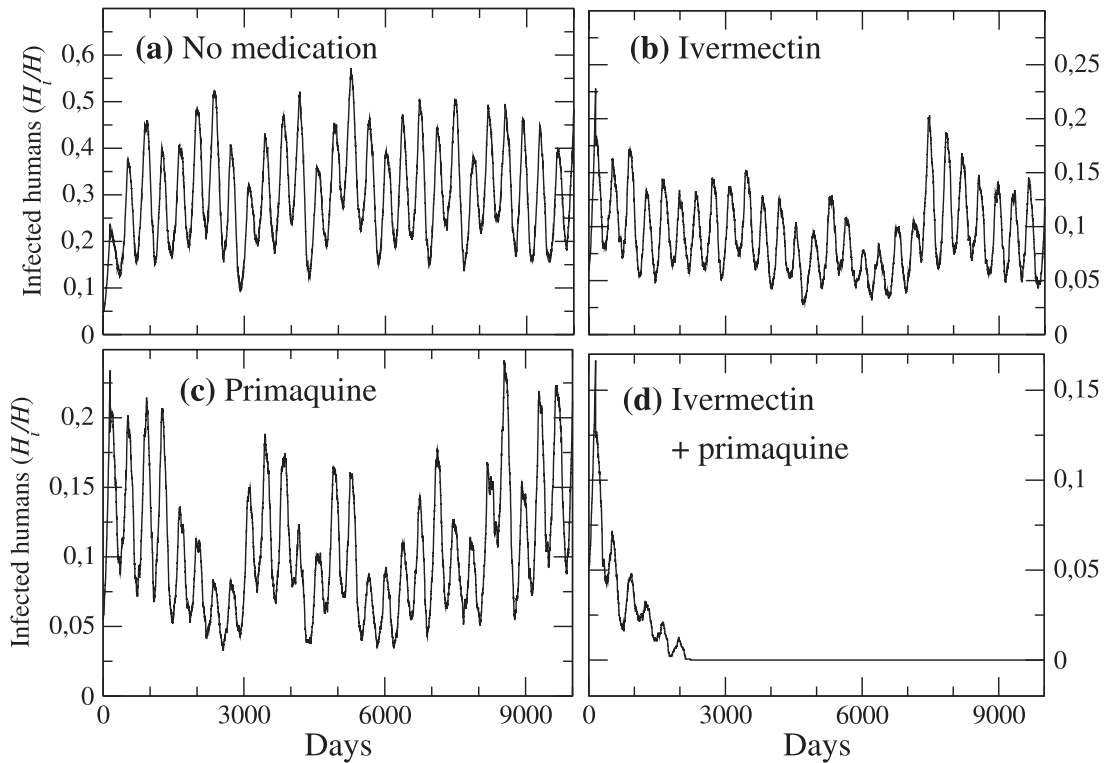


**Fig. 5.** (a) The evolution of the number of infected humans in an epidemic status with  $w_h = 0.6$  with  $p_{iv} = 0$ . (b) Application of ivermectin treatment with  $p_{iv} = 0.05$  to the situation shown in (a), keeping positive gametocytemia at  $w_h = 0.6$ . (c) Application of gametocytemia reduction with primaquine from  $w_h = 0.6$  to  $w_h = 0.467$ , without ivermectin ( $p_{iv} = 0$ ). (d) Combined gametocytemia reduction with primaquine and ivermectin treatment in epidemic status, with  $w_h = 0.467$  with  $p_{iv} = 0.05$ .

man fraction with ivermectin is approximately  $p_{iv} = 0.058$ . Higher  $p_{iv}$  values induce faster disease eradication scenarios. Similarly to Eq. (8), the step function can be modelled through the function

$$F_{iv}(p_{iv}) = 1 - \frac{1}{1 + \left(\frac{p_{iv}^{(t)}}{p_{iv}}\right)^{\alpha_{iv}}} \quad (10)$$

The fitting parameters here are  $p_{iv} = 0.058$  and  $\alpha_{iv} = 15$ .

Comparison of Figs. 3a and 4a, indicates that a more intensive use of ivermectin in the human population is qualitatively equivalent to a shorter gametocytemia time needed to maintain disease prevalence. The outcome of massive administration of ivermectin in a fraction of the human population reveals strong correlation with an effective reduction on the duration of positive gametocytemia. Consequently, both the probability of ivermectin treatment  $p_{iv}$  and annual malaria incidence are anticorrelated, as shown in Fig. 4b. Here, we run 10 simulations for each value of  $p_{iv}$  ranging from 0.020 to the value 0.058, which corresponds to the obtained critical value at the phase transition in Fig. 4a. The linear regression in Fig. 4b yields

$$I_{mal_{p_{iv}}} = 97 - 1509p_{iv} \quad (11)$$

with a Pearson correlation of  $r^2 = 0.9499$  and a  $p$ -value of  $P < .001$ . Similarly as what we discussed above for Eq. (9), here we observe positive incidence only for values of ivermectin  $p_{iv} \lesssim 97/1509 \lesssim p_{iv}^{(t)}$ .

### 3.3. Combined use of gametocidal agents and ivermectin: a copula approach for predicting optimal administration intensities

As shown in the previous Section 3.2, in a stable epidemic status, with 90 days of positive gametocytemia ( $w_h = 0.60$ ), after the use of ivermectin in 5% of the human population, there is a reduction in the fraction of infected human hosts. Compare Fig. 5a with

Fig. 5b. However, this reduction is not robust enough to achieve complete disease eradication. Similarly, after a reduction in the days of positive gametocytemia, namely from 90 to 70 days, with no ivermectin treatment, there is a weakening in disease transmission, although also not robust enough to achieve eradication (see Fig. 5c). But combining both effects, namely with a gametocytemia reduction from 90 to 70 days and ivermectin preventive treatment in 5% of the population, disease eradication is rapidly attained (Fig. 5d).

Apparently, the combination of these separate strategies may lead to a stronger action in suppressing malaria infection in the human population. Our quantitative analysis however provides a framework for deriving an estimation of how strong these strategies should be, when used in combination, in order to achieve full disease eradication. Assuming both factors to be independent from each other, a first order approximation to estimate the number of infected humans would be  $\hat{H} = F_g(w_h)F_{iv}(p_{iv})H$  and eradication would be the region in parameter space ( $w_h, p_{iv}$ ) satisfying

$$F_g(w_h)F_{iv}(p_{iv}) < \frac{1}{H}. \quad (12)$$

The fact that the time period of the parasite development in the mosquito is generally longer than 10 days (see Table 1), may explain the reason for the effectiveness of ivermectin in preventive campaigns directed to other endemic parasites in Africa. However, this effect may not be only related to an overall reduction in the number of mosquitoes, but also to a selective interference in the process of parasite development towards sporozoite inside the mosquito, and a preferential killing of infected mosquitoes. Therefore, both factors are correlated and the prediction presented above is biased towards a worst-case scenario.



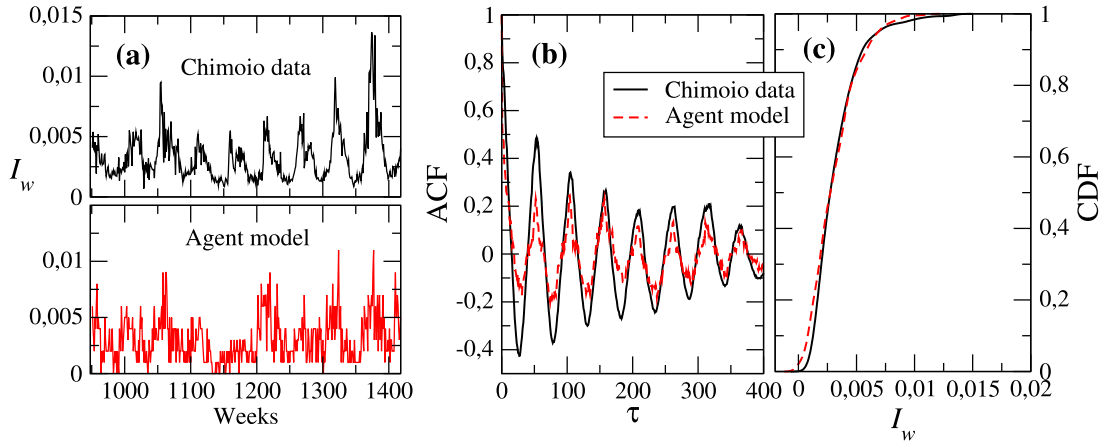


**Fig. 6.** (a) Time series of weekly malaria incidence  $I_w$ , comparing empirical data from Ref. (Ferrão et al., 2017a) (top) against data from one realization of the agent model (bottom), where 64 days of gametocytemia was used ( $w_h = 0.427$ ). (b) Auto-correlation function of the weekly malaria incidence from the empirical data (solid line), compared with the auto-correlation from the agent model simulation. (c) Cumulative density functions (CDF) of the malaria incidence for both empirical and simulation sets of data. In all cases  $p_{iv} = 0$ .

**4. Model validation and consistency tests: comparison with malaria transmission in chimoio**

In this section, we validate the agent model simulations against empirical data, namely time series at weekly intervals collected at Chimoio region in Mozambique (Ferrão et al., 2017a). In this African region, malaria is endemic revealing a trend, which increases during the four to five months of the wet season (high transmission season) and decreases during the rest of the year (low transmission season). The empirical time series includes a total of 490 561 malaria cases in a population of  $H = 324816$  human individuals, recorded from January 1st 2006 to December 31st 2014. During these 9 years, weekly malaria incidence  $I_w$  was analyzed in both the empirical set of data and in simulated data generated by the agent model. Fig. 6a shows both time series during 9 years (468 weeks).

From the total time of 30 years covered by the simulation, we discarded the first 14 weeks in order to weaken the influence of the initial conditions and to synchronize seasonality with Mozambique empirical data. Considering total simulation time, we have used three partial 468 weeks' time series (from weeks 15 to 482, 483 to 950 and 951 to 1418) which were very similar in global behavior (data not shown). For presentation purposes we have used the last one of these 3 time-series (from week 951 to 1418), revealing good correlation between our model and Mozambique empirical data, as in the horizontal axis label of Fig. 6a. The reason for excluding so many years of data was related to the necessity of using a time gap identical to the one of Mozambique empirical series (468 weeks). Since we scaled both populations to a maximum number of individuals, we neglect here demographic effects, which stand as a good approximation, as long as the human population density thus not exceed the radius of activity of individual mosquitoes.<sup>7</sup>

The simulation uses 64 days of positive gametocytemia ( $w_h = 0.427$ ), which relates to a marginally higher human-to-mosquito disease transmission efficiency, than that found at phase transition (cf. Fig. 3a). This validation procedure only relates to the trans-

mission model, not including therapeutic interventions with ivermectin or primaquine.

In Fig. 6b we plot the auto-correlation functions of the empirical data and of the simulation. The autocorrelation is defined as

$$\gamma(\tau) = \frac{\langle (I_w(t + \tau) - \bar{I}_w)(I_w(t) - \bar{I}_w) \rangle}{\sigma_{I_w}^2}, \tag{13}$$

where  $\bar{I}_w$  and  $\sigma_{I_w}^2$  are respectively the mean and variance of the incidence series and  $\langle \cdot \rangle$  represents the average over time  $t$ . Apart from a deviation of the local extremes, the periodicity of the simulated scenario matches rather well with the real seasonal oscillation period ( $\sim 1$  year). To quantify the similarity between real data and agent model simulation with computed the usual performance metrics, namely the mean absolute error (MAE)

$$MAE = \frac{1}{n} \sum_{t=1}^n |\hat{I}_w(t) - I_w(t)| \tag{14}$$

with  $\hat{I}_w(t)$  and  $I_w(t)$  representing the simulated and real incidence value and  $n = 468$  (weeks), the mean absolute percentual error (MAPE)

$$MAPE = \frac{1}{n} \sum_{t=1}^n \left| \frac{\hat{I}_w(t) - I_w(t)}{I_w(t)} \right| \tag{15}$$

and the root mean square error

$$RMSE = \left[ \frac{1}{n} \sum_{t=1}^n (\hat{I}_w(t) - I_w(t))^2 \right]^{1/2}. \tag{16}$$

The computation yields MAE= 0.00152, MAPE= 0.558 and RMSE=  $9.54 \times 10^{-5}$ . The simulation is within fluctuations of 50% of real incidence values.

We also compare the distribution of simulated and real incidence values, as plotted in Fig. 6c: the cumulative distributions match rather well, with a small Kolmogorov-Smirnov score (0.22) having a  $p$ -value smaller than 0.001.

Importantly, in all simulations, mosquito and human infection is strongly related, showing a similar oscillatory pattern. Moreover, only a small fraction of the mosquito population survived beyond the parasite development in the mosquito (10 days), which leads to a strong correlation between endemic prevalence in humans and mosquitoes in all endemic scenarios (McKenzie and Bossert, 2005).

Our model assumes rules based on classical and neoclassical assumptions, including several parameters from the classical

<sup>7</sup> In realistic conditions, mosquito population size is usually an unknown parameter, with spatial heterogeneous distribution according to topography, vegetation and water conditions for larval breeding. Consequently, it can only be guessed as an approximation, resulting from data obtained with the help of mosquito traps and larval water count in water reservoirs, or indirectly from counting mosquito bites.

**Table 2**

Classical Ross parameters from theory and model simulation for endemic scenario A, close to phase transition, i.e. with 68 days of gametocytemia ( $w_h = 0.453$ ). The two main quantities, reproductive number  $R_0$  and the annual entomological inoculation rate  $EIR$ , are within the classical theoretical values.

Description	Theory	Model
Basic reproductive number ( $R_0$ )	<b>1.619</b>	<b>0.973</b>
Annual entom. inoculation rate ( $EIR$ )	<b>0.961</b>	<b>0.965</b>
Fraction of infected mosquitoes ( $m$ )	2	2
Human feeding rate ( $a$ )	0.238	0.239
Sporozoite rate ( $Z$ )	—	0.006
Force of infection ( $\lambda$ )	0.47	0.284
Mosquito-to-Human transmission ( $b$ )	0.18	0.108
Human-to-Mosquito transmission ( $c$ )	0.091	0.090
Human recovery rate ( $q_h$ )	0.011	0.011
Mosquito daily mortality ( $q_m$ )	0.1	0.1

Ross–Macdonald model (Ross, 1915; Macdonald, 1957; Smith and McKenzie, 2004). The two main quantities in this classical model are the annual entomological inoculation rate  $EIR$ , which is defined as the number of bites per year on a human host from an infectious mosquito, and the reproductive number  $R_0$ , which represents the number of infected humans generated from one single infectious mosquito in a population of susceptible and non-immune individuals.

For evaluation of our model, we compare the values obtained in our simulations with the expected theoretical ones, which are given in Refs. Ross (1915); Smith and McKenzie (2004). Results are given in Table 2. For estimating the annual entomological inoculation rate we use the definition

$$EIR = 365 m a Z, \quad (17)$$

where  $m$  is the mosquito density (number of mosquitoes per human individual,  $m = \frac{N_m}{N_h}$ ),  $a$  is the human feeding rate given by (see Table 1 and Section 2),  $a = (p_Q n_b (1 - u) s) / \tau_s$ , and  $Z$  is the sporozoite rate (fraction of infectious mosquitoes). For estimating the reproductive number, we use the Ross definition (Ross, 1915)

$$R_0 = \frac{ma^2bc}{q_h q_m}, \quad (18)$$

where  $b$  is the mosquito-to-human transmission efficiency,  $b = k_h (1 - \bar{v})$ ,  $c$  is the human-to-mosquito transmission efficiency,  $c = k_m w_h$ , and  $q_h$  and  $q_m$  are given by Eqs. (1) and (2) respectively. As indicated in Table 2, the expected theoretical values of both these quantities are well reproduced by the simulations. The lower value of  $R_0$  in the simulation, when compared with Ross theory is due to the fact that the  $b$  value in the simulation only takes into account bites from infectious mosquitoes.

## 5. Discussion and conclusion: towards medical strategies

We introduce an agent model for assessing the effect of gametocytemia and drug administration in epidemiological scenarios of malaria. Our model was calibrated by considering various aspects of the disease dynamics and supported by field data. We uncover the existence of a phase transition between an absorption state with disease eradication and an endemic/epidemic regime.

Because several parameters from our model were based on the Mozambique epidemic environment, validation of the model implementation took place by the comparison with field collected data series for malaria incidence in the typical seasonal endemic malaria region of Chimoio, Mozambique. Importantly, this field data time-series covered a long time period of malaria incidence, namely 9 years (Ferrão et al., 2017a). Although the parameter values in Table 1 are case-dependent, they are within the range of typical values described in the literature.

In complex models, phase transition stands as a critical concept of stochastic simulation. Its precise definition is useful to identify the occurrence of state transition between disease eradication and endemic stability, which can be used for better preventive planning. At critical equilibrium points, malaria transmission dynamics was defined taking into account the predicted rational use of anti-malarial strategies in the near future.

Special attention was given to the role of gametocytemia in human-to-mosquito transmission. All our model simulations assumed the duration of positive gametocytemia to be in the range of 0.387 to 0.733 of total infection time. With a small variation in gametocytemia prevalence it was possible to define all tested transition phases. These small changes in gametocytemia were considered as a model for effective gametocidal treatment, such as the administration of primaquine or methylene blue (Karl et al., 2011; Kuehn and Pradel, 2010; Eziefula et al., 2012; Sutanto et al., 2013; John, 2016; Gonçalves et al., 2016; Lin et al., 2017). Transition phases were clearly defined, promoting a better understanding of the disease dynamics, as well as of the points of sudden stochastic transition from epidemic prevalence to disease eradication.

In the present model, we also analyzed preventive intervention with ivermectin, a well-known agent with capability of interfering with human-to-mosquito transmission. An intervention with ivermectin may be highly selective in targeting recently infected mosquitoes, killing the mosquito before the complete development of the parasite in the mosquito. This aspect bears no relation to gametocytemia prevalence (Chaccour et al., 2010; Kobylinski et al., 2012; Ouédraogo et al., 2015). Apparently, the role of mosquito mortality from ivermectin in disease transmission does not significantly overlap with the effect of gametocidal drug intervention.

However, notice that, in this model, the action of primaquine is based on its general properties as a gametocidal agent. For simplicity, we have assumed gametocytemia duration reduction in *Plasmodium falciparum* as the main drug effect, neglecting its action on other forms of *Plasmodium*. Methylene blue can be taken as an alternative and as a potential gametocidal agent, but our model intends to catch general spreading regimes and therefore, we did not focus on any other major drug characteristics. Moreover, while the results may be encouraging, showing that ivermectin coverage as low as 5–10% can have a high impact, a next step should be in the direction of considering the pharmacokinetics of this drug which could afterwards provide insight on how this prolonged coverage could be achieved with the current formulations. The detailed biochemical mechanisms that trigger gametocytogenesis in *Plasmodium* are not well known. However, this process may be influenced by host immunity and anti-malaria therapy (Karl et al., 2011; Kuehn and Pradel, 2010). For human-to-mosquito transmission to be effective, male and female stage V gametocytes must be present in the blood during mosquito feeding. Once inside mosquito midgut, gametocytes will mature to gametes promoting fertilization and maturation to zygote stage, ookinete, oocyst, and finally to the sporozoite, the infectious form of the parasite present in mosquito salivary glands. Common gametocidal drug agents (primaquine, artemisinin and methylene blue (Eziefula et al., 2012; Sutanto et al., 2013; John, 2016; Gonçalves et al., 2016; Lin et al., 2017; Peatey et al., 2009; Bosson-Vanga et al., 2018)) usually fail to act in the early stages of gametocyte maturation. But their inhibitory action on Gametocytes in stage V may be very effective in reducing the time of gametocytemia duration (Kuehn and Pradel, 2010).

Vector control, by itself, is not enough to eradicate disease transmission. Long standing cyclic positive gametocytemia in a few human individuals may perpetuate transmission for a long time and more attention should be directed towards human disease

reservoirs as possible hot-spots for chronic mosquito infection. Preventing mosquito infection from these hot-spot human reservoirs by reducing the time of positive gametocytemia with the help of a selective mosquito-killing-after-bite preventive drug strategy with ivermectin, may turn out to be a more effective strategy in the fight against malaria.

The combined intervention of gametocidal agents and ivermectin may also be useful in reducing pressure in areas where drug resistance is becoming a major problem as a result of new mutations in the background of mass drug administration (Dondorp et al., 2010; Dama et al., 2017). Our results seem to indicate that such a theoretical possibility may deserve serious consideration in future malaria prevention campaigns.

Dynamical aspects of human therapy with drug agents such as artemisinin or quinine (with specific intervention in disease status and gametocytemia probability), population heterogeneity and human migration were not included in the present analysis. Model simulations assumed the existence of a typical and isolated African village with limited drug availability.

Our computational model allowed us to test the combined use of different preventive interventions with antimalarial agents like ivermectin (killing mosquitoes during parasite's development) or primaquine (gametocytemia reduction) that could significantly influence disease outcome, and therefore contribute to a better knowledge of disease transmission dynamics in different endemic scenarios. With the present model, it is possible to recreate simulations for different disease regions with specific seasonality conditions, and to anticipate events as a result of selective interventions in certain human subgroups in all simulations.

From the main findings of this work, a set of valuable insights are possible. First, in endemic locations, small differences in gametocytemia prevalence in human populations, obtained from preventive intervention in a small fraction of the population with gametocidal drugs (Eziefula et al., 2012; Sutanto et al., 2013; John, 2016; Gonçalves et al., 2016; Lin et al., 2017; Peatey et al., 2009), may result in very different outcomes, despite the relative stability of classical human-to-mosquito infectiousness parameter  $c$ .

Second, the demonstrated mosquitocidal properties of ivermectin in the first days after a mosquito feed, may potentiate the effect of gametocidal agents with drastic interference in human-to-mosquito transmission efficiency. This preventive action may also benefit from its combined use with LLIN/ITN/IRS.

Third, our model indicates that with a combined ivermectin and primaquine scissor-like intervention, malaria eradication may be possible in a small African village after a short period of time.

## Acknowledgments

We thank Miguel Prudêncio (IMM - Lisbon) for his help in defining model parameters, and for his crucial remarks in discussing the model design.

## References

- Alout, H., Krajacich, B., Meyers, J., et al., 2014. Evaluation of ivermectin mass drug administration for malaria transmission control across different west african environments. *Malar. J.* 13 (1), 1–10.
- Annan, K., Mukinay, C.D., 2017. Stability and time-scale analysis of malaria transmission in human-mosquito population. *Int. J. Syst. Sci. Appl. Math.* 2017 2 (1), 1–9.
- Aregawi, M., Lynch, M., Bekele, W., et al., 2014. Time series analysis of trends in malaria cases and deaths at hospitals and the effect of antimalarial interventions, 2001–2011, ethiopia. *PLoS One* 9 (11), 2001–2011.
- Bombliès, A., Duchemin, J., Elthair, E., 2009. A mechanistic approach for accurate simulation of village scale malaria transmission. *Malar. J.* 8, 223.
- Bosson-Vanga, H., Franetich, J., Soulard, V., et al., 2018. Differential activity of methylene blue against erythrocytic and hepatic stages of plasmodium. *Malar. J.* 17 (1), 143.
- Bretscher, M., Maire, N., Felger, I., Owusu-Agyei, S., Smith, T., 2015. Asymptomatic plasmodium falciparum infections may not be shortened by acquired immunity. *Malar. J.* 14, 294.
- Chaccour, C., Lines, J., Whitty, C., 2010. Effect of ivermectin on anopheles gambiae mosquitoes fed on humans: the potential of oral insecticides in malaria control. *J. Infect. Dis.* 202 (1), 113–116.
- Chitnis, N., Hardy, D., Smith, T., 2012. A periodically-forced mathematical model for the seasonal dynamics of malaria in mosquitoes. *Bull. Math. Biol.* 74 (5), 1098–1124.
- Chitnis, N., Schapira, A., Schindler, C., Penny, M., Smith, T., 2018. Mathematical analysis to prioritise strategies for malaria elimination. *J. Theor. Biol.* 455, 118–130.
- Coffeng, L., Hermsen, C., Sauerwein, R., de Vlas, S., 2017. The power of malaria vaccine trials using controlled human malaria infection. *PLOS Comp. Biol.* 13 (1), e1005255.
- Dama, S., Niangaly, H., Ouattara, A., et al., 2017. Reduced ex vivo susceptibility of plasmodium falciparum after oral artemether-lumefantrine treatment in mali. *Malar. J.* 16 (1), 59.
- DePina, A., Niang, E., Andrade, A., et al., 2018. Achievement of malaria pre-elimination in cape verde according to the data collected from 2010 to 2016. *Malar. J.* 17 (1), 236.
- Depinay, J., Mbogo, C., Killeen, G., et al., 2004. A simulation model of african anopheles ecology and population dynamics for the analysis of malaria transmission. *Malar. J.* 3 (1), 29.
- Dietz, K., Molineaux, L., Thomas, A., 1974. A malaria model tested in the african savannah. *Bull. World Health Organ.* 50 (3–4), 347–357.
- Dondorp, A., Yeung, S., White, L., et al., 2010. Artemisinin resistance: current status and scenarios for containment. *Nat. Rev. Microbiol.* 8 (4), 272–280.
- Doolan, D., Dobano, C., Baird, J., 2009. Acquired immunity to malaria. *Clin. Microbiol. Rev.* 22 (1), 13–36.
- Eckhoff, P., 2011. A malaria transmission-directed model of mosquito life cycle and ecology. *Malar. J.* 10, e303.
- Erment, V., Fink, A.H., Jones, A.E., Morse, A.P., 2011. Development of a new version of the liverpool malaria model. i. refining the parameter settings and mathematical formulation of basic processes based on a literature review. *Malar. J.* 10 (1), 35.
- Ewing, D., Cobbold, C., Purse, B., Nunn, M., White, S., 2016. Modelling the effect of temperature on the seasonal population dynamics of temperate mosquitoes. *J. Theor. Biol.* 400, 65–79.
- Eziefula, A., Gosling, R., Hwang, J., et al., 2012. Rationale for short course primaquine in africa to interrupt malaria transmission. *Malar. J.* 11 (1), 360.
- Felger, I., Maire, N., Bretscher, M., et al., 2012. The dynamics of natural plasmodium falciparum infections. *PLoS One* 7 (9), e45542.
- Ferrão, J., Mendes, J., Painho, M., 2017. Modelling the influence of climate on malaria occurrence in chimoio municipality, mozambique. *Parasites Vectors* 10 (1), 1–12.
- Ferrão, J., Mendes, J., Painho, M., Zacarias, S., 2017. Malaria mortality characterization and the relationship between malaria mortality and climate in chimoio, mozambique. *Malar. J.* 1–9.
- Filipe, A.N., Riley, E.M., Drakeley, C.J., Sutherland, C.J., Ghani, A.C., 2007. Determination of the processes driving the acquisition of immunity to malaria using a mathematical transmission model. *PLoS Comput. Biol.* 3 (12), e255.
- Gaudart, J., Touré, O., Dessay, N., et al., 2009. Modelling malaria incidence with environmental dependency in a locality of sudanese savannah area, mali. *Malar. J.* 8, 61.
- Gerardin, J., Ouédraogo, A., McCarthy, K., Eckhoff, P., Wenger, E., 2015. Characterization of the infectious reservoir of malaria with an agent-based model calibrated to age-stratified parasite densities and infectiousness. *Malar. J.* 1–13.
- Gonçalves, B., Tiono, A., Ouédraogo, A., et al., 2016. Single low dose primaquine to reduce gametocyte carriage and plasmodium falciparum transmission after artemether-lumefantrine in children with asymptomatic infection: a randomised, double-blind, placebo-controlled trial. *BMC Med.* 14 (1), 40.
- Gurarie, D., Karl, S., Zimmerman, P., King, C., St.Pierre, T., Davis, T., 2012. Mathematical modeling of malaria infection with innate and adaptive immunity in individuals and agent-based communities. *PLoS One* 7 (3), e34040.
- Hasyim, H., Dhimal, M., Bauer, J., Montag, D., Groneberg, D.A., Kuch, U., Müller, R., 2018. Does livestock protect from malaria or facilitate malaria prevalence? a cross-sectional study in endemic rural areas of indonesia. *Malar. J.* 17 (1), 302.
- Jindal, A., 2017. Agent-based modeling and simulation of mosquito-borne disease transmission. In: *Proc. 16th Int. Conf. Auton. Agents Multiagent Syst. - AAMAS*.
- John, C., 2016. Primaquine plus artemisinin combination therapy for reduction of malaria transmission: promise and risk. *BMC Med.* 14, 65.
- Kamgang, S., Tchoumi, J.C., 2015. A model of the dynamic of transmission of malaria, integrating SEIRS, SEIS, SIRS and SIS organization in the host-population. *J. Appl. Anal. Comput.* 5 (4), 688–703.
- Karl, S., Gurarie, D., Zimmerman, P., King, C., St.Pierre, T., Davis, T., 2011. A sub-microscopic gametocyte reservoir can sustain malaria transmission. *PLoS One* 6 (6), e20805.
- Kaufmann, C., Briegel, H., 2004. Flight performance of the malaria vectors anopheles gambiae and anopheles atroparvus. *J. Vector Ecol.* 29 (1), 140–153.
- Killeen, G.F., Govella, N.J., Lwetoijera, D.W., Okumu, F.O., 2016. Most outdoor malaria transmission by behaviourally-resistant anopheles arabiensis is mediated by mosquitoes that have previously been inside houses. *Malar. J.* 15 (1), 225.
- Kobylynski, K., Foy, B., Richardson, J., 2012. Ivermectin inhibits the sporogony of plasmodium falciparum in anopheles gambiae. *Malar. J.* 11 (1), 381.
- Kobylynski, K., Sylla, M., Chapman, P., Sarr, M., Foy, B., 2011. Ivermectin mass drug administration to humans disrupts malaria parasite transmission in senegalese villages. *Am. J. Trop. Med. Hyg.* 85 (1), 3–5.

- Koella, J., 1991. On the use of mathematical models of malaria transmission. *Acta Trop.* 49 (1), 1–25.
- Korenromp, E., Mahiané, G., Hamilton, M., Pretorius, C., Cibulskis, R., Lauer, J., Smith, T.A., Briët, O.J.T., 2016. Malaria intervention scale-up in africa: effectiveness predictions for health programme planning tools, based on dynamic transmission modelling. *Malar. J.* 15 (1), 417.
- Kuehn, A., Pradel, G., 2010. The coming-out of malaria gametocytes. *J. Biomed. Biotechnol.* 976827, 1–11.
- Laurens, M.B., Billingsley, P., Richman, A., Eappen, A.G., Adams, M., Li, T., Chakravarty, S., Gunasekera, A., Jacob, C.G., Sim, B.K.L., Edelman, R., Plowe, C.V., Hoffman, S.L., Lyke, K.E., 2013. Successful human infection with *p. falciparum* using three aseptic anopheles stephensi mosquitoes: a new model for controlled human malaria infection. *PLoS One* 8 (7), e68969.
- Lee, P., Liu, C., Rampao, H., Rosario, V., Shaio, M., 2010. Pre-elimination of malaria on the island of príncipe. *Malar. J.* 9, 26.
- Lin, J., Lon, C., Spring, M., et al., 2017. Single dose primaquine to reduce gametocyte carriage and plasmodium falciparum transmission in cambodia: an open-label randomized trial. *PLoS One* 12 (6), e0168702.
- Lloyd, A.L., May, R.M., 1996. Spatial heterogeneity in epidemic models. *J. Theor. Biol.* 179, 1–11. (March 1995).
- Lyke, K.E., Laurens, M., Adams, M., Billingsley, P.F., Richman, A., Loyevsky, M., Chakravarty, S., Plowe, C.V., Sim, B.K.L., Edelman, R., Hoffman, S.L., 2010. Plasmodium falciparum malaria challenge by the bite of aseptic anopheles stephensi mosquitoes: results of a randomized infectivity trial. *PLoS One* 5 (10), e13490.
- Macdonald, G., 1957. The epidemiology and control of malaria. Oxford University Press.
- Mandal, S., Sarkar, R., Sinha, S., 2011. Mathematical models of malaria - a review. *Malar. J.* 10, 202.
- McKenzie, F., Bossert, W., 2005. An integrated model of plasmodium falciparum dynamics. *J. Theor. Biol.* 232 (3), 411–426.
- Mendes, A., Albuquerque, I., Machado, M., Pissarra, J., Meireles, P., Prudêncio, M., 2017. Inhibition of plasmodium liver infection by ivermectin. *Antimicrob. Agents Chemother.* 61 (2), 1–8.
- Ngonghala, C., Mohammed-Awel, J., Zhao, R., Prosper, O., 2016. Interplay between insecticide-treated bed-nets and mosquito demography: implications for malaria control. *J. Theor. Biol.* 397, 179–192.
- Ngonghala, C.N., Valle, S.Y.D., Zhao, R., Mohammed-Awel, J., 2014. Quantifying the impact of decay in bed-net efficacy on malaria transmission. *J. Theor. Biol.* 363, 247–261.
- Ngwa, G., Shu, W., 2000. A mathematical model for endemic malaria with variable human and mosquito populations. *Math. Comput. Model.* 32 (7–8), 747–763.
- Omura, S., Crump, A., 2017. Ivermectin and malaria control. *Malar. J.* 16 (1), 1–3.
- Organization, W.H., 2013. Malaria entomology and vector control. World Health Organization Tech. rep.
- Organization, W.H., 2018. World malaria report. Tech. rep. World Health Organization.
- Ouédraogo, A., Bastiaens, G., Tiono, A., et al., 2015. Efficacy and safety of the mosquitocidal drug ivermectin to prevent malaria transmission after treatment: a double-blind, randomized, clinical trial. *Clin. Infect. Dis.* 60 (3), 357–365.
- Pagès, F., Houze, S., Kurtkowiak, B., Balleydier, E., Chieze, F., Filleul, L., 2018. Status of imported malaria on réunion island in 2016. *Malar. J.* 1–11.
- Peatey, C., Skinner-Adams, T., Dixon, A., McCarthy, J., Gardiner, D., Trenholme, K., 2009. Effect of antimalarial drugs on plasmodium falciparum gametocytes. *J. Infect. Dis.* 200, 1518–1521.
- Ross, R., 1915. Some a priori pathometric equations. *Br. Med. J.* 1 (2830), 546–547.
- Sarkar, R., Chatterjee, C., 2017. Application of different time series models on epidemiological data - comparison and predictions for malaria prevalence. *SM J. Biom. Biostat.* 2 (4), 1022.
- Smith, D., McKenzie, F., 2004. Statics and dynamics of malaria infection in anopheles mosquitoes. *Malar. J.* 3, 13.
- Smith, N.R., Trauer, J.M., Gambhir, M., Richards, J.S., Maude, R.J., Keith, J.M., Flegg, J.A., 2018. Agent-based models of malaria transmission: a systematic review. *Malar. J.* 17 (1), 1–16.
- Stanley, H.E., 1971. Introduction to Phase Transitions and Critical Phenomena. Oxford University Press.
- Sutanto, I., Suprijanto, S., Kosasih, A., et al., 2013. The effect of primaquine on gametocyte development and clearance in the treatment of uncomplicated falciparum malaria with dihydroartemisinin-piperazine in south sumatra, western indonesia: an open-label, randomized, controlled trial. *Clin. Infect. Dis.* 56 (5), 685–693.
- Tyrrell, M., Verdonck, K., Muela, S., Gryseels, C., 2017. Defining micro-epidemiology for malaria elimination : systematic review and meta-analysis. *Malar. J.* 1–20.
- White, L., Maude, R., Pongtavornpinyo, W., et al., 2009. The role of simple mathematical models in malaria elimination strategy design. *Malar. J.* 8 (1), 212.